TÜBİTAK

Turkish J. Eng. Env. Sci.
34 (2010) , 215 – 230.

doi:10.3906/muh-1004-127

Cracks in base-restrained plain and reinforced concrete walls

Kheira OUZAA, Mohammed Benali BENMANSOUR
Faculty of Architecture and Civil Engineering, University of Sciences and Technology Mohamed Boudiaf, BP 1505 El M'Naouer, 31000 Oran-ALGERIA
e-mail: kh_ouzaa@yahoo.fr

Received 28.04.2010

Abstract

This study deals with the problem of shrinkage cracks in reinforced concrete walls restrained at the base. A finite element model to study cracking of the wall was proposed. Nonlinear behavior of concrete was considered by means of a smeared crack approach. The equations proposed by ACI Committee 209 were used to model the mechanical properties of concrete, as well as the average concrete shrinkage within the thickness of the wall. It was found that the suggested model closely predicts the true behavior of cracking in base-restrained concrete walls, including the crack pattern and crack propagation.

Key Words: Wall, reinforced concrete, horizontal reinforcement, shrinkage, cracking

Introduction

Volume changes due to shrinkage are significantly important because, in practice, these movements are usually partly or wholly restrained; therefore, they induce stresses. Once the tensile strength of the concrete is exceeded, a crack will develop.

Cracks in concrete are undesirable because they are unsightly. They impair structural durability, increase permeability, and reduce strength.

The control of shrinkage cracks in reinforced concrete walls has been investigated by many researchers. Carlson and Reading (1988) developed a technique for determining shrinkage stresses in concrete building walls using rubber models. Kheder et al. (1994) studied the problem of cracking due to volume change of base-restrained reinforced concrete walls. Their crack prediction formula is based on the theory of change in restraint during the crack formation. Stoffers (1978) presented the problem of cracking due to shrinkage and temperature variation in walls. He based his derivations on the fact that the crack spacing in base-restrained concrete walls is determined by the effect of the restraining base and not by any reinforcement that may be present in the wall. Kheder et al. (1990) presented the strategic reinforcement for controlling volume change cracking in base-restrained concrete walls. Their works are based on the use of finite element analysis to obtain the diagrams of distribution of restraint factor in walls with different length-to-height ratios. These diagrams are used to determine the amount and the distribution of steel reinforcement in a position effective for controlling cracking. Kianoush et al. (2008) studied the cracking behavior of reinforced concrete walls under restrained volumetric deformations using the computer program ABAQUS/6.4, which is an FE-based program.

The objective of the present work was to study the phenomenon of shrinkage cracks in base-restrained plain and reinforced concrete walls.

A finite element method was developed and used to find the degree of restraint, sequence, and distribution of cracks and the effect of the horizontal reinforcement (HR) of the wall using a rectangular 4-node element. The suggested model includes material nonlinearity, smeared crack representation, tension stiffening, stress degradation of concrete in the parallel crack direction, and shear retention of concrete on the cracked surface.

Concrete Representation

Reinforced concrete walls were modeled by 4-node rectangular elements using the following polynomial functions for the assumed displacement field:

$$u = \alpha_1 + \alpha_2 x + \alpha_3 y + \alpha_4 xy \tag{1}$$

$$v = \alpha_5 + \alpha_6 x + \alpha_7 y + \alpha_8 xy \tag{2}$$

where u and v are the displacement in (x) and (y) directions, and α_1, α_2, α_3, α_4, α_5, α_6,α_7, and α_8 are the coefficients of the displacement field.

Prior to cracking, the concrete was assumed to be isotropic, homogenous, and linearly elastic; thus, the stress-strain relations for the plane stress were:

$$\left\{ \begin{array}{c} \sigma_x \\ \sigma_y \\ \tau_{xy} \end{array} \right\} = \frac{E_c(t)}{1-\nu^2} \left(\begin{array}{ccc} 1 & \nu & 0 \\ \nu & 1 & 0 \\ 0 & 0 & \frac{1-\nu}{2} \end{array} \right) \left\{ \begin{array}{c} \varepsilon_x \\ \varepsilon_y \\ \gamma_{xy} \end{array} \right\} \tag{3}$$

in which σ_x, σ_y, and τ_{xy} are the stresses of concrete in global coordinates; ε_x, ε_y, and γ_{xy} are the strains of concrete in global coordinates; $E_c(t)$ is the modulus of elasticity of concrete at time t; and υ is Poisson's ratio of concrete.

ACI Committee 209 (ACI, 1990) proposed the equations for predicting the compressive strength $f'_c(t)$, direct tensile strength $f'_t(t)$, and modulus of elasticity $E_c(t)$ at time t:

$$f'_c(t) = \frac{t}{4 + 0.85t} f'_c(28) \tag{4}$$

$$f'_t(t) = 0.007\sqrt{w f'_c}(t) \tag{5}$$

$$E_c(t) = 0.043 w^{1.5} \sqrt{f'_c}(t) \tag{6}$$

where $f'_c(28)$ is the 28-day compressive strength, w is the concrete unit weight in kg/m^3, and $f'_c(t), f'_t(t)$, and $E_c(t)$ are measured in MPa.

Smeared crack representations treat concrete as an orthotropic material with principal axes normal and parallel to the crack direction (Figure 1).

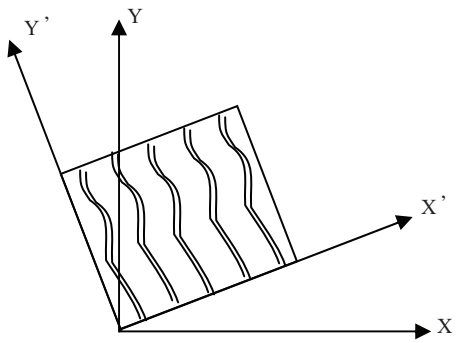

Figure 1. Coordinates system for cracks.

The incremental stress-strain relationship associated with the crack coordinates (Eq. (3)) becomes:

$$\left\{ \begin{array}{c} \Delta\sigma_{x'} \\ \Delta\sigma_{y'} \\ \Delta\tau_{x'y'} \end{array} \right\} = \left(\begin{array}{ccc} 0 & 0 & 0 \\ 0 & E_t & 0 \\ 0 & 0 & \mu G \end{array} \right) \left\{ \begin{array}{c} \Delta\varepsilon_{x'} \\ \Delta\varepsilon_{y'} \\ \Delta\gamma_{x'y'} \end{array} \right\}. \tag{7}$$

In Eq. (7), the modulus of elasticity of concrete is reduced to 0 in the direction normal to the crack direction, and E_t is the tangent modulus of concrete parallel to the crack direction. Poisson's ratio is taken as 0 due to the lack of interaction between the 2 orthogonal directions. $G = \frac{E_c}{2}$ is the shear modulus of cracked concrete, and μ is the shear retention factor with $0 < \mu \leq 1$ (Finite Element Analysis of Reinforced Concrete, 1982). A constant value of $\mu = 0.25$ was used in this study.

The stress in a reinforced concrete wall restrained at the base varies from point to point in accordance with the variation in degree of restraint throughout the wall. When this stress reaches the tensile strength of the concrete, a crack will initiate at the base, where the restraint is greatest, and progress upward until a point is reached at which the stress is insufficient to continue the crack. After initial cracking, the tension caused by restraint in the region of the crack is redistributed to the uncracked element of the wall, thereby increasing the tensile stresses above the crack. The residual stress is computed as the difference between the stresses existing prior to cracking and stresses that the element can sustain at the same strain level after cracking. A load vector equivalent to this residual stress is then computed for each cracked element according to:

$$\{P\} = \int_{vol} [B]^T \{\sigma\}\, dvol \tag{8}$$

where $\{\sigma\}$ is the residual stress vector and $[B]$ is the conventional nodal displacement strain matrix.

Tension Stiffening

The use of the orthotropic constitutive equation to represent cracked concrete may not be totally realistic, because the cracked concrete of a reinforced concrete element can still carry some tensile stress in the direction normal to the crack. This phenomenon is termed "tension stiffening" (ACI, 2001). In this work, a general tension stiffening curve suggested by Bhide (1986) was used. This curve can be expressed as follows:

$$f_t = \frac{f'_t}{1 + 1000\varepsilon_t(\phi/90)^{1.5}} \tag{9}$$

where f_t and ε_t are respectively the average tensile stress and the average tensile strain normal to the crack direction, f'_t is the maximum tensile strength of concrete, and Φ is measured in degrees counterclockwise from the steel direction to the crack direction.

Stress Degrading Effect for Concrete Parallel to the Crack Direction

After cracking has taken place, the concrete parallel to the crack direction is still capable of resisting either tensile or compressive forces. When it is subjected to tension, a pure linear elastic behavior is assumed (Figure 2), and E_t is taken as $E_c(t)$ in Eq. (7). On the other hand, when concrete is subjected to compression, experimental results (Vecchio and Collins, 1982; Maekawa and Okamura, 1983) show that the tensile cracks cause damage to the concrete with the transverse tensile strain, having a degrading effect not only on the compressive strength but also on the compressive stiffness.

Several formulas (Vecchio and Collins, 1982; Cervenka, 1985; Vecchio and Collins, 1986) have been proposed to determine the degraded maximum compressive strength f_{cm} for concrete parallel to the crack direction. The experimentally determined relationship suggested by Vecchio and Collins (1986) was used in this study:

$$\frac{f_{cm}}{f'_c} = \frac{1}{0.8 + 0.34\frac{\varepsilon_t}{\varepsilon_0}} \leq 1 \tag{10}$$

where ε_0 is the strain corresponding to the maximum concrete compressive strength f'_c. After the peak strength f_{cm} is determined, the stress-strain curve suggested by Saenz (1964) is used to calculate the concrete compressive stress f_c:

$$f_c = \frac{E_c\varepsilon}{1 + (R + R_E - 2)\frac{\varepsilon}{\varepsilon_0} - (2R-1)\left(\frac{\varepsilon}{\varepsilon_0}\right)^2 + R\left(\frac{\varepsilon}{\varepsilon_0}\right)^3} \tag{11}$$

where

$$R = \frac{R_E(R_\sigma - 1)}{(R_\varepsilon - 1)^2} - \frac{1}{R_\varepsilon}, R_E = \frac{E_c}{E_0}, E_0 = \frac{f_{cm}}{\varepsilon_0}, R_\sigma = 4, R_\varepsilon = 4 \tag{12}$$

in which R and R_E are the ratio relation and the modulus ratio, E_0 is the secant modulus of elasticity at f_c for concrete, and R_σ and R_ε are respectively the stress and strain ratio.

The tangent modulus E_t used in Eq. (7) can be found by differentiating Eq. (11):

$$E_t = \frac{df_c}{d\varepsilon} = \frac{E_c\left[1 + (2R-1)\left(\frac{\varepsilon}{\varepsilon_0}\right)^2 - 2R\left(\frac{\varepsilon}{\varepsilon_0}\right)^3\right]}{\left[1 + (R + R_E - 2)\left(\frac{\varepsilon}{\varepsilon_0}\right) - (2R-1)\left(\frac{\varepsilon}{\varepsilon_0}\right)^2 + R\left(\frac{\varepsilon}{\varepsilon_0}\right)^3\right]^2}. \tag{13}$$

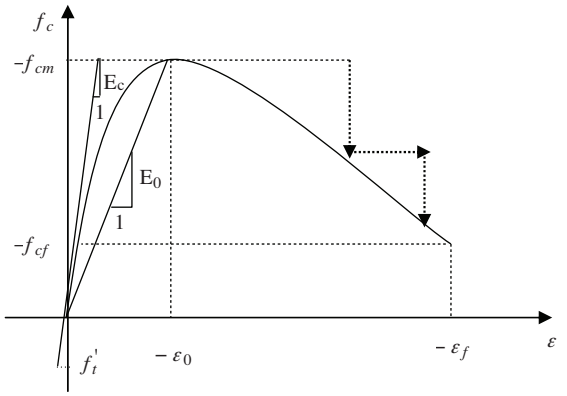

Figure 2. Stress-strain curve for concrete parallel to the crack direction.

Reinforced Concrete Representation

The material stiffness of the composite element is obtained by superposition of the material stiffness of the individual material components, concrete and reinforcement.

A stress-strain relationship for the element can be written in the following form (Chen, 1982):

$$\{\sigma_t\} = [D]\,\{\varepsilon_t\} \tag{14}$$

where the total stress vector $\{\sigma_t\}$ and the total strain vector $\{\varepsilon_t\}$ can be defined as follows:

$$\{\sigma_t\} = \left\{ \begin{array}{c} \sigma_x \\ \sigma_y \\ \tau_{xy} \end{array} \right\} \text{ and } \{\varepsilon_t\} = \left\{ \begin{array}{c} \varepsilon_x \\ \varepsilon_y \\ \gamma_{xy} \end{array} \right\}. \tag{15}$$

$[D]$ is the composite material stiffness matrix. The strains are similar for the 2 components, steel and concrete, while the total stress vector is the sum of the component stress vectors:

$$\{\sigma_t\} = \{\sigma_c\} + \sum_{i=1}^{N} \{\sigma\}_i \tag{16}$$

where $\{\sigma_c\}$ is the concrete stress vector and $\{\sigma\}_i$ is the stress vector for the ith steel layer.

Stresses $\{\sigma_t\}$, $\{\sigma_c\}$, and $\{\sigma\}_i$ act on the unit area of the composite cross section. It can be noted that the total stresses $\{\sigma_t\}$ do not represent real stresses, but rather internal forces acting on a composite element. These stresses can be found from the strain as follows:

$$\{\sigma_c\} = [D_c]\,\{\varepsilon_t\} \tag{17}$$

$$\{\sigma\}_i = [D]_i\,\{\varepsilon_t\} \tag{18}$$

in which $[D_c]$ is the material stiffness matrix for the concrete component and $[D]_i$ is the material stiffness matrix for the ith steel layer. By substituting Eqs. (17) and (18) into Eq. (16), and then comparing Eq. (14) with Eq. (16), the total material stiffness matrix can be evaluated as follows:

$$[D] = [D_c] + \sum_{i=1}^{N} [D]_i. \tag{19}$$

The stress-strain curve of reinforcing steel is modeled by an idealized bilinear curve identical in tension and compression (Figure 3). The incremental constitutive matrix for the ith steel layer, $[D]_i$, can be written as:

$$[D]_i = \begin{pmatrix} \rho_i E_S & 0 & 0 \\ 0 & 0 & 0 \\ 0 & 0 & 0 \end{pmatrix} \tag{20}$$

where ρ_i and E_s are respectively the steel percentage for the ith steel layer and the modulus of elasticity of steel.

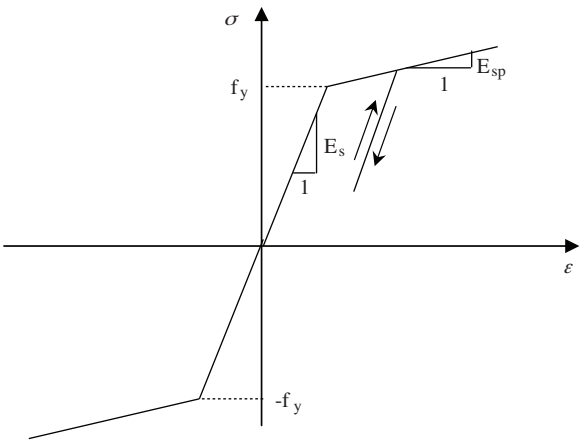

Figure 3. Idealized stress-strain curve for steel.

Nonlinear Solutions Procedures

In a simple linear elastic system, the fundamental approach of the solution is the solving technique of a set of algebraic equations for the unknown displacements $\{d\}$ of the form:

$$[K_G]\{d\} = \{F\} \tag{21}$$

in which $[K_G]$ and $\{F\}$ are the stiffness matrix and the vector of external force, respectively.

The above procedure cannot be accomplished in the case of a nonlinear system, in which the stiffness matrix $[K_G]$ is a function of material properties and structural displacement. The solution for a nonlinear problem (Mercer and Palazotto, 1987) is usually attempted by a step-by-step method, a constant stiffness method, or a combination of both. In the latter procedure, the load is applied incrementally, and, with each increment, successive iterations are performed for more accurate results. Depending on the sequence of the stiffness matrix computation, the combined method can be classified into 2 forms. The full Newton-Raphson form is the first form, in which the stiffness matrix is continually updated during each iteration. The second form is the modified Newton-Raphson, in which the stiffness matrix is computed at the beginning of each load step and remains constant during iterations until reaching convergence.

The modified Newton-Raphson method has been widely used in nonlinear analysis of reinforced concrete structure and was adopted in this study.

Convergence criteria

The iterative technique used in the present problem was to decide whether the current iteration was sufficiently close to the exact solution. The convergence criteria for nonlinear structural problems can usually be classified as displacement convergence and force convergence.

The force convergence criterion was adopted in this work, supposing that the first cracks appear when the concrete load reaches its ultimate value (nonlinear elastic behavior). The violation of equilibrium is estimated by the magnitude of the residual unbalanced nodal forces, which are calculated during each iteration as follows (Aldstedt and Bergan, 1978):

$$\{\Delta f\} = \{F\} - \{I\} \tag{22}$$

where $\{\Delta f\}$ is the vector of residual unbalanced nodal force, $\{F\}$ is the applied load vector, and $\{I\}$ is the internal force vector, which depends on the nodal deformations $\{d\}$.

The convergence formula is:

$$\frac{\left[\sum_{j=1}^{NEQ} (\Delta f)^2\right]^{1/2}}{\left[\sum_{j=1}^{NEQ} (F)^2\right]^{1/2}} \leq \text{ Force tolerance} \tag{23}$$

in which NEQ represents the number of equations (Mercer and Palazotto, 1987). The force tolerance used in the present work was taken as equal to 0.05.

Mathematical Formulation of Shrinkage

According to ACI Committee 209 (ACI, 1990), the shrinkage strain occurring between t_0 at the start of shrinkage and t can be predicted using the following formula:

$$\varepsilon_{sh}(t) = \frac{(t - t_0)}{35 + (t - t_0)} \varepsilon_{shu} \tag{24}$$

where ε_{shu} is the ultimate shrinkage and represents the product of the applicable correction factors:

$$\varepsilon_{shu} = 780 \gamma_{sh} 10^{-6} \tag{25}$$

$$\gamma_{sh} = \gamma_h \gamma_t \gamma_s \gamma_c \gamma_\varphi \gamma_\alpha \tag{26}$$

where $\gamma_h, \gamma_t, \gamma_s, \gamma_c, \gamma_\varphi$ and γ_α are empirical coefficients that take into consideration the effects of humidity, minimum member thickness, slump, cement content, fine aggregate percentage, and air proportion, respectively. γ_h is expressed by:

$$\begin{array}{l} \gamma_h = 1.4 - 0.01h \text{ for } 40\% \leq h \leq 80\% \\ \gamma_h = 3.0 - 0.03h \text{ for } 80\% \leq h \leq 100\% \end{array} \tag{27}$$

where h is the relative humidity (%).

$$\begin{array}{l} \gamma_t and \gamma_s \text{ are determined by} \\ \gamma_t = 1.23 - 0.0015 T_h \text{ for the duration of shrinkage } \leq 1 \text{ year} \end{array} \tag{28}$$

where T_h is the minimum member thickness (mm), and

$$\gamma_s = 0.89 + 0.00161S \tag{29}$$

where S is the slump of fresh concrete (mm).

$$\begin{array}{l} \gamma_c \text{ is determined by} \\ \gamma_c = 0.75 + 0.00061C \end{array} \tag{30}$$

where C is the cement content (kg/m^3).
γ_φ and γ_α are expressed by

$$\begin{array}{l} \gamma_\varphi = 0.3 + 0.014\varphi \text{ for } \varphi \leq 50\% \\ \gamma_\varphi = 0.9 + 0.002\varphi \text{ for } \varphi > 50\% \end{array} \tag{31}$$

where φ is the ratio of the fine aggregate to the total aggregate (%), and

$$\gamma_\alpha = 0.95 + 0.008\alpha \tag{32}$$

where α is the air content (%).

Results and Discussion

In this section, the finite element program is applied to represent shrinkage cracks in base-restrained members.

The following properties were assumed in the analysis: $w = 2359\,\text{kg/m}^3$, $f'_c = 37.2\,\text{MPa}$, $f'_t = 2.07$ MPa, $\text{E}_c = 30$ GPa, $\nu = 0.15$, and $\text{E}_s = 200$ GPa.

In all walls, the percentage of the vertical steel reinforcement and diameter of the bar were taken as equal to 0.5% and 8 mm, respectively.

The walls were assumed to be completely fixed to their foundation and 1 m long (Figure 4). The thickness of the walls and the duration of drying were taken as equal to 0.1 m and 30 days, respectively.

The data required for applying the ACI Committee 209 equations (ACI, 1990) to predict shrinkage values are given in Table 1.

Table 1. Shrinkage correction factor γ_{sh}.

t_0 (days)	h (%)	T_h (mm)	S (mm)	C (kg/m^3)	ϕ (%)	α (%)	γ_{sh}
7	40	100	50	350	38.5	4	0.83

Degree of restraint

The degree of restraint in a wall with a restrained, continuous base varies within the member. At the bottom, the wall is fully restrained, and at the top, it is more or less free to move.

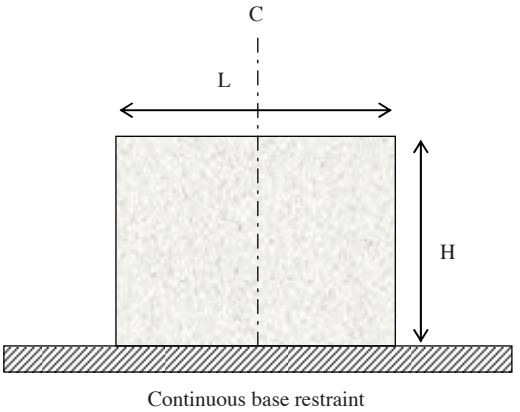

Figure 4. Geometry of the reinforced concrete wall.

The first crack usually occurs at the mid-length of the wall, since the restraint is highest at this position. As each new crack forms at approximately the midpoint of the uncracked portions of the base, the previously formed cracks will propagate vertically.

The mid-length point of the wall at the base has a maximum degree of restraint. Figure 5 shows the degree of restraint at this position of the walls for L/H = 1. The degree of restraint K_R is calculated during analysis as the ratio of restrained shrinkage strain $\varepsilon_r(t)$ to free shrinkage strain $\varepsilon_{sh}(t)$:

$$K_R = \frac{\varepsilon_r(t)}{\varepsilon_{sh}(t)}. \tag{33}$$

The restrained shrinkage strain is determined by subtracting the free shrinkage strain from the total strain.

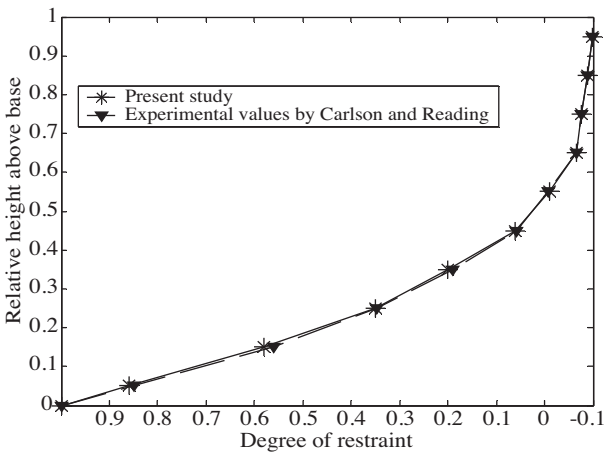

Figure 5. Degree of restraint at center section of wall for L/H = 1.

Models made of rubber were used by Carlson and Reading (1988) to study drying shrinkage stress conditions in base-restrained walls with different shapes, with and without openings, and with different degrees of restraint. Degree of restraint contour diagrams in walls with different length-to-height ratios of 1, 2, 3, 4, 5, 6, 7, 8, 9, 10, and 20 were prepared. These diagrams were used for comparison with the results of the finite element analysis. The values of the degree of restraint calculated in the present study were found to be in good

agreement with the experimental values obtained by Carlson and Reading (1988). Small negative values of the degree of restraint were found at the wall top, indicating the occurrence of small compressive stresses.

Figure 6 shows the percentage of increase in the degree of restraint with different reinforcement ratios at relative levels of the wall above the base for L/H = 1. From this figure, it is obvious that the contribution of reinforcement to restraint is very limited at the level nearest to the base, and it increases toward the top of the wall.

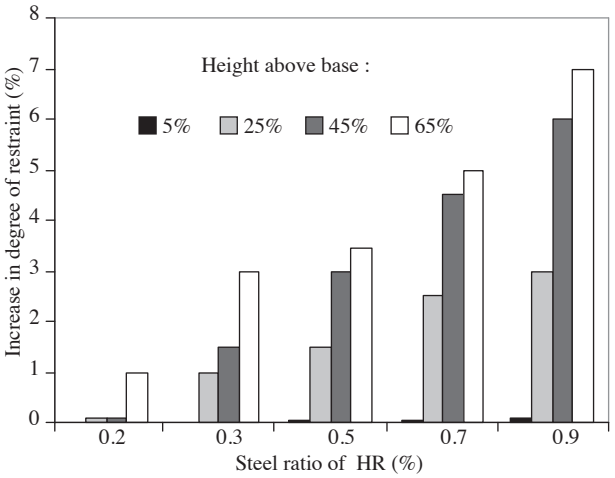

Figure 6. Increase in degree of restraint with different horizontal steel ratios for L/H = 1.

Sequence of cracking

The first crack was noticed to happen exactly at the mid-length point of the wall. After formation of the first crack, the degree of restraint changed and its maximum value occurred at approximately the mid-length point of the 2 uncracked portions at the base level. A maximum degree of restraint took place above the crack level due to the redistribution of stresses. Hence, the first crack propagated and new cracks initiated at approximately the mid-length of the uncracked portions of the wall. This sequence of cracking is shown in Figures 7 and 8. This process was repeated for the second, third, and following cracks.

Crack analysis

Figure 9 gives the values of concrete shrinkage strains and steel stresses in cracked elements (Figures 7 and 8) of the wall with different horizontal steel ratios.

In the present analysis, steel reinforcement carried a compression stress before cracking. This stress was dependent on the degree of base restraint and the sequence of crack formation. At the bottom level, where the degree of restraint is high, the compressive stress in steel is relatively low and increases upward. After cracking, the tensile stress carried by concrete transfers to steel reinforcement in the vicinity of the crack. The value of this transferred tensile stress is affected by the degree of base restraint and the number of cracks at that level.

As can be seen above, the presence of steel reinforcement did not affect the time of first crack initiation, whereas it intentionally affected the sequence and pattern of crack propagation.

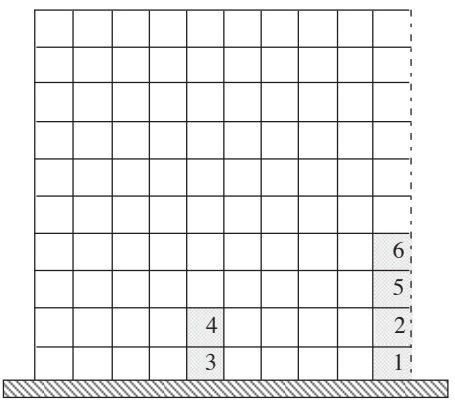

(a)

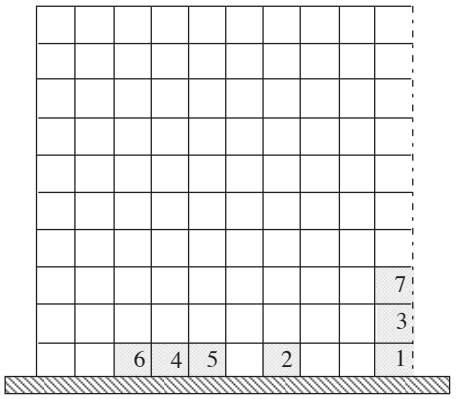

(b)

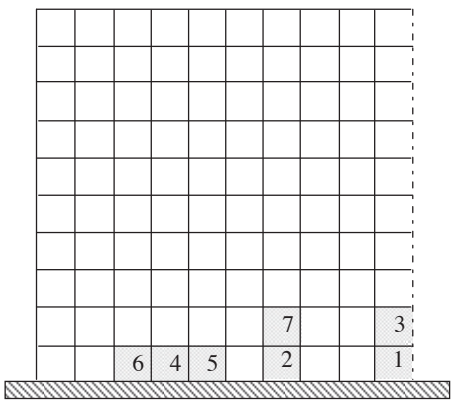

(c)

Figure 7. Sequence of crack propagation for HR = a) 0%, b) 0.2 %, c) 0.3 %, d) 0.5 %, e) 0.7 %, and f) 0.9%.

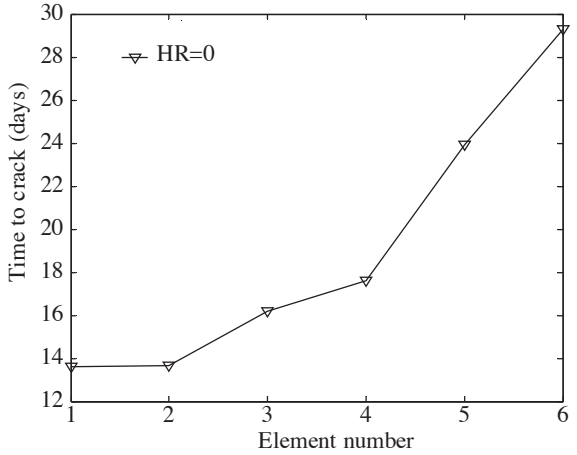

(a)

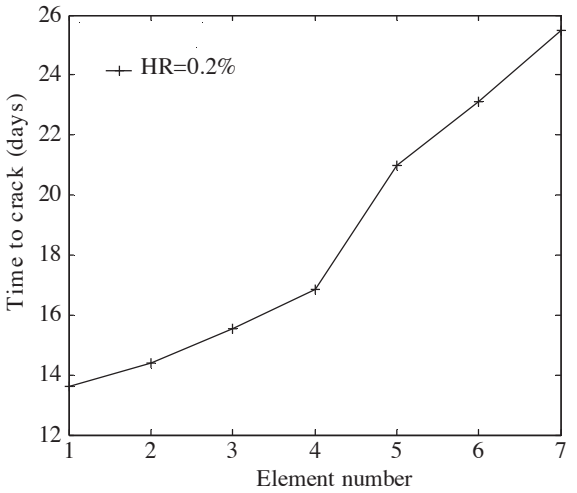

(b)

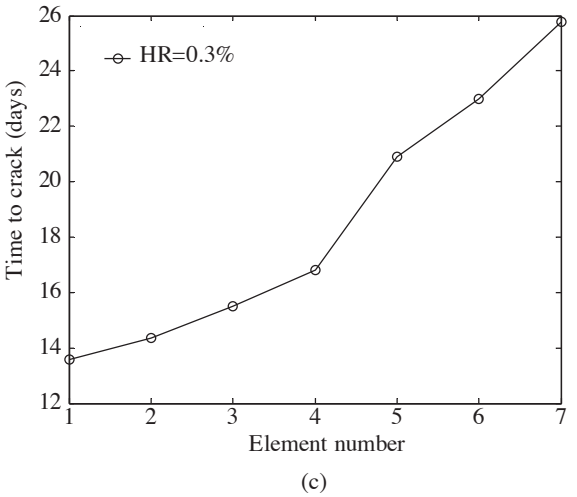

(c)

Figure 8. Time to crack of elements for HR = a) 0%, b) 0.2%, c) 0.3%, d) 0.5%, e) 0.7 %, and f) 0.9%.

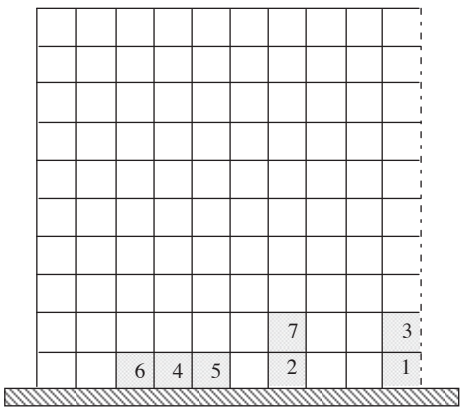

(d)

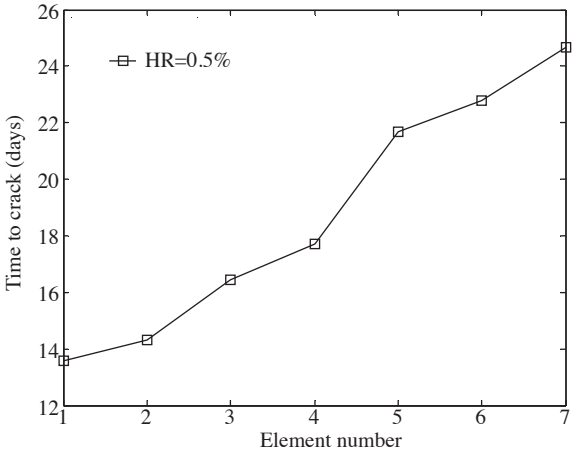

(d)

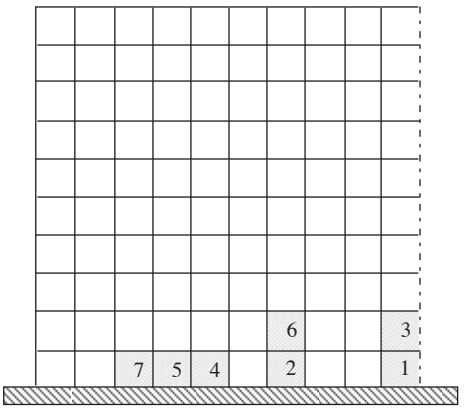

(e)

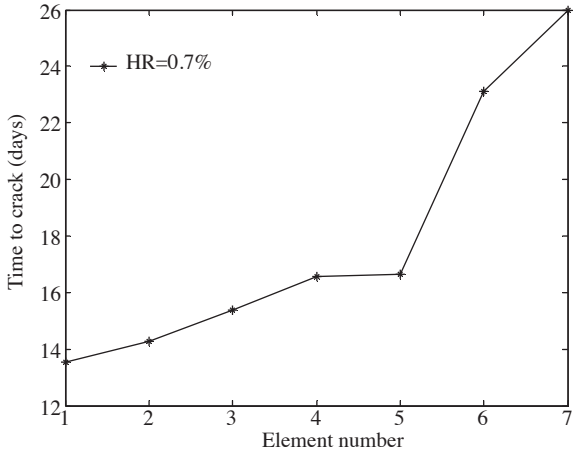

(e)

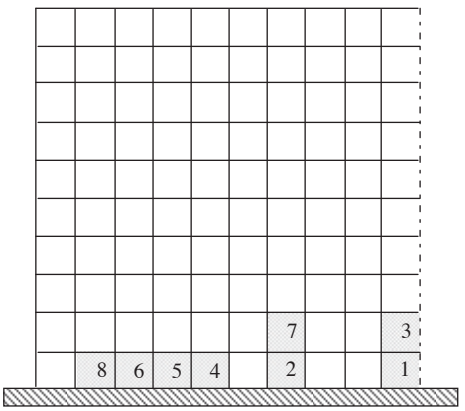

(f)

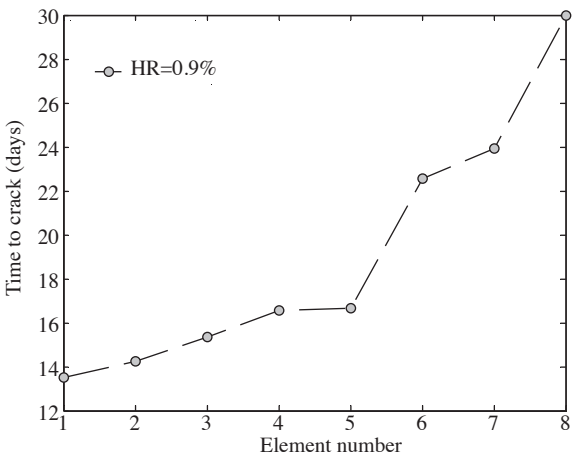

(f)

Figure 7. Continued.

Figure 8. Continued.

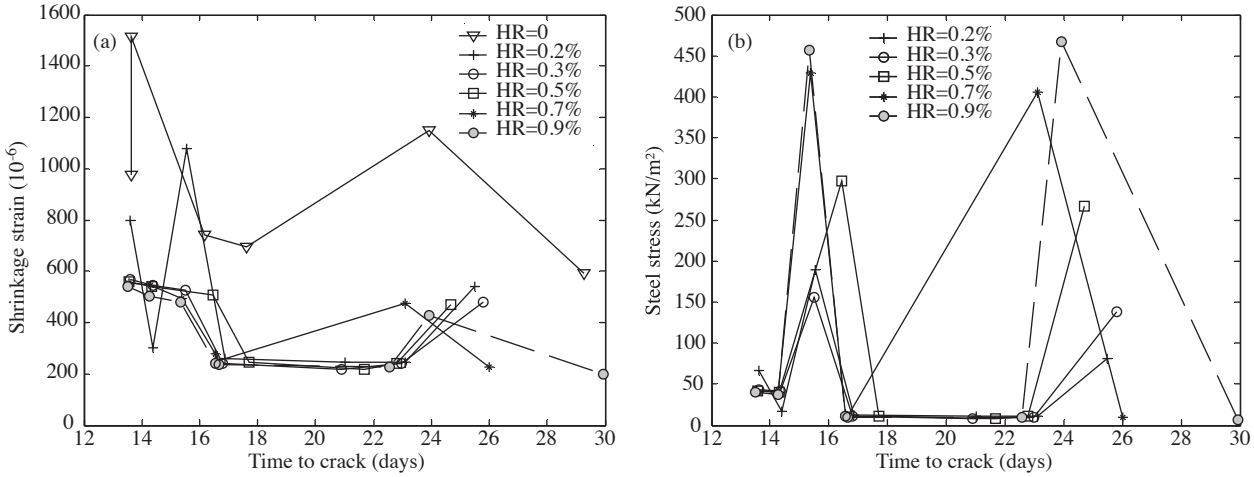

Figure 9. In cracked elements of the wall, a) concrete shrinkage strains and b) steel stresses.

Figure 10 shows the relationship between time and percentage of crack height. There it is clear that the existence of steel reinforcement delays the propagation of any crack, which permits others cracks to initiate on both sides of that crack. It can be seen that an increase in the horizontal steel ratio will cause a decrease in the height of cracks at the end of the drying period studied.

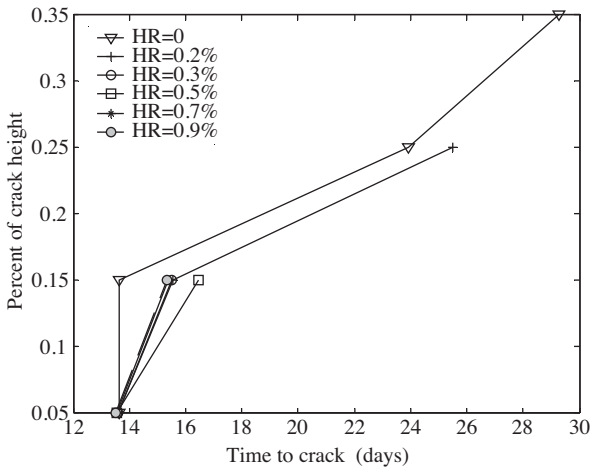

Figure 10. Crack propagation of the wall.

The crack width at any level in the wall is simply a function of the amount of the tensile strain formerly carried by concrete and relieved by the process of cracking. In other words, the crack width at any level of the wall is proportional to the difference between the restrained shrinkage strain and the tensile strain capacity of concrete.

The width of a single crack and the spacing between the primary cracks are affected by discretization, which means that a smaller element size results in a smaller crack width and in distances between cracks. The values of crack width given in Figure 11 were calculated by multiplying the element width by the strain, which is calculated in the center of the cracked element.

From comparing the values of width at different levels, it can be seen that the crack width increased to a certain level above the base, and that it decreased upward until it took the lowest value at the tip of the crack.

The change of crack width throughout the height of the wall indicates that the reinforcement ratio must be increased in an ascending pattern toward the base.

The steel reinforcement allowed the opening of more, but finer, cracks (Figures 11 and 12). Hence, it decreased the spacing and width of cracks.

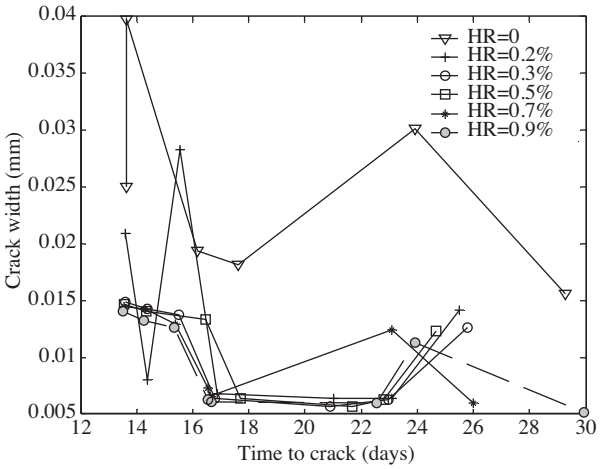

Figure 11. Effect of the horizontal reinforcement ratio on crack width.

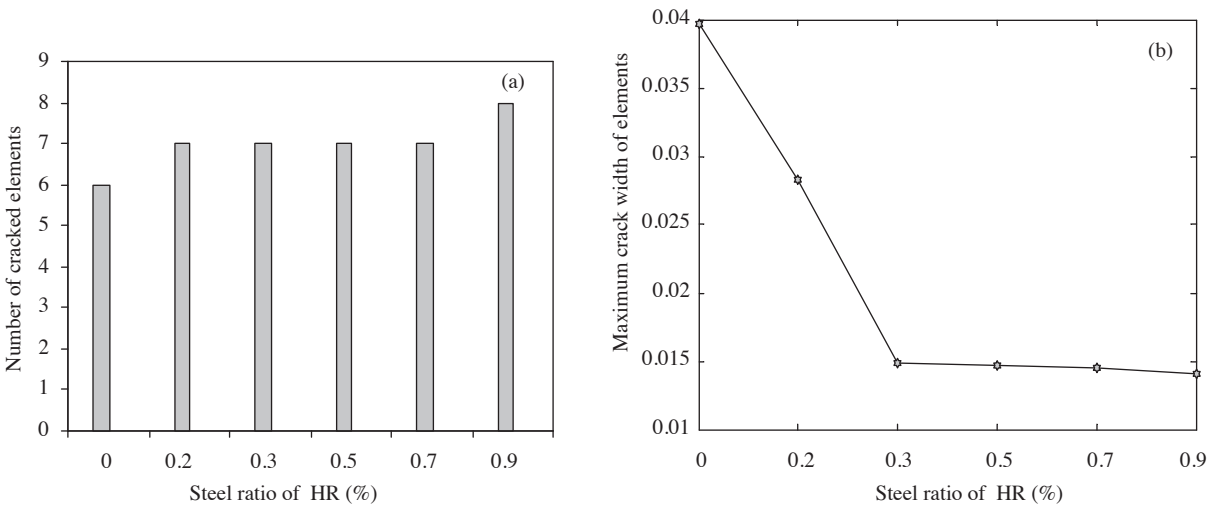

Figure 12. For different horizontal steel ratios, a) number of cracked elements and b) maximum crack width of elements.

Table 2 gives the crack widths calculated according to the present finite element procedure and according to Kheder's equations (Kheder et al., 1994):

$$W_{\max} = S_{\max} \left[C_1 \left(R_b - C_2 R_a \right) e_v - {}^{e_{ult}}/_2 \right] \tag{34}$$

$$S_{\max} = \frac{2kdH}{kd + \rho H} \tag{35}$$

where W_{max} is the maximum crack width, S_{max} is the maximum crack spacing, C_1 is the coefficient for creep effect and is taken equal to 0.6, C_2 is the coefficient for slippage between the base and the wall and is taken equal to 0.8 (the value estimated from crack width measurements at the level immediately above the restraining base), e_v is the total volumetric shrinkage, e_{ult} is the elastic tensile strain capacity of the concrete, R_a is the degree of restraint after cracking, R_b is the degree of restraint before cracking, k is the constant depending on bar type (k = 0.57 for deformed steel bars), d is the bar diameter, ρ is the steel reinforcing ratio, and H is the height of the wall. The values of e_v and e_{ult} were obtained from the finite element analysis used in this study.

From Table 2, it can be seen that there was relatively good agreement between the values of crack width from the 2 approaches.

Table 2. Width of crack versus relative crack height with different horizontal steel ratios.

			Crack width (mm)	
	HR (%)	Relative height of crack (%)	Kheder $C_1 = 0.6$, $C_2 = 0.8$ $e_v = 288 \times 10^{-6}$, $e_{ult} = 150 \times 10^{-6}$ k = 0.57	Present study
L/H = 1	0	5	0.0316	0.0250
		15	0.0315	0.0397
		25	0.0276	0.0301
		35	0.0145	0.0155
	0.2	5	0.0211	0.0209
		15	0.0279	0.0283
		25	0.0141	0.0142
	0.3	5	0.0153	0.0149
		15	0.0140	0.0137
	0.5	5	0.0151	0.0147
		15	0.0129	0.0133
	0.7	5	0.0169	0.0147
		15	0.0168	0.0129
	0.9	5	0.0140	0.0141
		15	0.0130	0.0126

Conclusions

The following conclusions were obtained from the results of the present study:

- The degree of restraint calculated in the present analysis is in good agreement with the degree of restraint estimated by Carlson and Reading. After each new crack initiation or old crack propagation, the degree of restraint is redistributed along the wall.
- The sequence of cracking showed good agreement with the limitations of cracking sequence stated by ACI Committee 209.
- The trend of cracking recognized in the present study is that the width of a primary crack is always greater than that of any secondary crack in the same wall. Furthermore, the first crack to form was found to be the widest one in the wall at any stage of drying.
- For economic purposes, crack width can be controlled by varying the steel distribution along the wall height according to the variation of crack width through its height.

References

ACI Committee 209, "Prediction of Creep, Shrinkage and Temperature Effects in Concrete Structures", American Concrete Institute Manual of Concrete Practice Part 1, Farmington Hills, Michigan, 1990.

ACI Committee 224, "Control of Cracking in Concrete Structures", American Concrete Institute, Farmington Hills, Michigan, 2001.

Aldstedt, E. and Bergan, P.G., "Nonlinear Time Dependent Concrete Frame Analysis", Journal of Structural Division, ASCE, 104, 1077-1092, 1978.

Bhide, S.B., "Reinforced Concrete Element in Shear and Tension", PhD Thesis, University of Toronto, 1986.

Carlson, R.W. and Reading, T.J., "Model Study of Shrinkage Cracking in Concrete Building Walls", ACI Structural Journal, 85, 395-404, 1988.

Cervenka, V., "Constitutive Model for Cracked Reinforced Concrete", ACI Journal, 82, 877-882, 1985.

Chen, W.F., "Plasticity in Reinforced Concrete", McGraw-Hill Book Company, New York, 1982.

"Finite Element Analysis of Reinforced Concrete," American Society of Civil Engineers, New York, 1982.

Kheder, G.F., Rawi, R.S.A. and Dhahi, J.K.A, "A Study of the Behavior of Volume Change Cracking in Base-Restrained Concrete Walls", Materials and Structures, 27, 383-392, 1994.

Kheder, G.F. and Fadhil, A.S., "Strategic Reinforcement for Controlling Volume-Change Cracking in Base-Restrained Concrete Walls", Materials and Structures, 23, 358-363, 1990.

Kianoush, M.R., Acarcan, M. and Ziari, A., "Behavior of Base Restrained Reinforced Concrete Walls under Volumetric Change", Engineering Structures, 30, 1526-1534, 2008.

Maekawa, K. and Okamura, H., "The Deformational Behavior of Constitutive Equation of Concrete Using the Elasto-Plastic and Fracture Model", Journal of the Faculty of Engineering - University of Tokyo, 39, 253-328, 1983.

Mercer, J.G. and Palazotto, A.N., "Elastic-Plastic Nonlinearities Considering Fracture Mechanics", Computers and Structures, 25, 919-935, 1987.

Saenz, L.P., "Discussion of 'Equation for the Stress-Strain Curve of Concrete' by Dessayi and Krishnan", ACI Journal, 61, 1229-1235, 1964.

Stoffers, H., "Cracking Due to Shrinkage and Temperature Variations in Walls", Heron, 1978.

Vecchio, F.J. and Collins, M.P., "The Response of Reinforced Concrete to In-Plane Shear and Normal Stresses", Department of Civil Engineering, University of Toronto, 1982.

Vecchio, F.J. and Collins, M.P., "The Modified Compression Field Theory for Reinforced Concrete Elements Subjected to Shear", ACI Journal, 83, 219-231, 1986.